



HAL
open science

Shifted Bernstein–Legendre polynomial collocation algorithm for numerical analysis of viscoelastic Euler–Bernoulli beam with variable order fractional model

Yuhuan Cui, Jingguo Qu, Cundi Han, Gang Cheng, Wei Zhang, Yiming Chen

► **To cite this version:**

Yuhuan Cui, Jingguo Qu, Cundi Han, Gang Cheng, Wei Zhang, et al.. Shifted Bernstein–Legendre polynomial collocation algorithm for numerical analysis of viscoelastic Euler–Bernoulli beam with variable order fractional model. *Mathematics and Computers in Simulation*, 2022, 200, pp.361-376. 10.1016/j.matcom.2022.04.035 . hal-04444998

HAL Id: hal-04444998

<https://hal.science/hal-04444998>

Submitted on 22 Jul 2024

HAL is a multi-disciplinary open access archive for the deposit and dissemination of scientific research documents, whether they are published or not. The documents may come from teaching and research institutions in France or abroad, or from public or private research centers.

L'archive ouverte pluridisciplinaire **HAL**, est destinée au dépôt et à la diffusion de documents scientifiques de niveau recherche, publiés ou non, émanant des établissements d'enseignement et de recherche français ou étrangers, des laboratoires publics ou privés.



Distributed under a Creative Commons Attribution - NonCommercial 4.0 International License

Shifted Bernstein-Legendre polynomial collocation algorithm for numerical analysis of viscoelastic Euler-Bernoulli beam with variable order fractional model

Yuhuan Cui¹ · Jingguo Qu^{1*} · Cundi Han² · Gang Cheng³ · Wei Zhang¹ · Yiming Chen^{2,3*} .

Received: date / Accepted: date

Abstract In this paper, a kinetic equation of Euler-Bernoulli beam is established with variable order fractional viscoelastic model. An effective numerical algorithm is proposed. This method uses a combination of shifted Bernstein polynomial and Legendre polynomial to approximate the numerical solution. The effectiveness of the algorithm is tested and verified by mathematical examples. The dynamic behavior of viscoelastic beams made of two materials under various loading conditions is studied.

Keywords Euler-Bernoulli beam · Variable order fractional model · Collocation method · Shifted Bernstein function · Shifted Legendre polynomial · Dynamic behavior

1 Introduction

Viscoelastic materials exhibit both elastic and viscous deformation under external loading conditions. They are considered as special damping materials, which play an important part in the vibration and noise reduction of equipment. Polyurea and Polyethylene terephthalate polymer (PET) are two of these viscoelastic materials. Polyurea has good abrasion resistance and thermal stability [1,2]. PET has good stability, low abrasion and high hardness, which is the greatest toughness among thermoplastics. It is mainly used for fibers, and a small amount is used for engineering plastics. This paper analyzes the mechanical behavior of these two viscoelastic materials.

*Corresponding author: Yiming Chen, Jingguo Qu
chenym@ysu.edu.cn, qujingguo@ncst.edu.cn

1 College of Science, North China University of Science and Technology, 063210, Tangshan, Hebei, China

2 School of Science, Yanshan University, 066004, Qinhuangdao, Hebei, China

3 INSA Centre Val de Loire, Univ. Tours, Univ. Orléans, LaMÉ, 3 rue de la chocolaterie, CS 23410, 41034 Blois, France

Viscoelastic models have been mainly used to describe material behavior in beam vibration research in recent years. The development of the constitutive viscoelastic models has attracted widely attention of scientific researchers. These models include differential constitutive relations [3–6]. Oskouie et al. [7] studied the vibrations of fractional viscoelastic Timoshenko nanobeams based on the Gurtin-Murdoch model. The effects of viscoelasticity coefficient and fractional order on the frequency and damping of vibrations of the beams were investigated. A variational finite difference method was proposed to solve the nonlocal vibrations of Euler-Bernoulli nanobeams within the framework of fractional calculus [8]. A fractional variational method was proposed to solve the governing equation of Bernoulli-Euler beam [9]. The influences of fractional order on the nonlinear bending and postbuckling responses with various boundary conditions were investigated. However, integer order models cannot describe dynamic viscoelastic behavior well. Therefore, fractional order was introduced into the viscoelastic constitutive model because it can accurately describe the characteristics of viscoelastic materials. Xu et al. [10] established a fractional order equation of a viscoelastic beam, and analyzed the dynamic behaviors and steady-state response of viscoelastic beam by wave method. Freundlich [11] studied the transient vibration of Euler-Bernoulli cantilever beam at both ends under fractional Kelvin Voigt model. Martin [12] developed an improved variational iterative method to analyze the simply supported viscoelastic beams with a fractional order Zener model. Fractional order models are proved to be more comprehensively for the description of the materials' viscoelastic behavior [13], especially for their time dependent mechanical properties. In variable fractional order models, the fractional order can be considered as a function of time, which makes the models more efficient to capture the dynamic response of the materials [14, 15].

However, in the analysis process, a small change will cause great changes in this system. Fractional order constitutive model unable accurately describe the dynamic behavior of viscoelastic materials in most cases. Variable order fractional operators show more sensitivity and accuracy in the numerical modelling in mechanical engineering [16]. Sun and Chen [17] numerically analyzed the viscoelastic columns under a variable order fractional model. Huang et al. [18] established a viscoelastic plastic model based on fractional calculus theory. The experimental data showed that the fractional order model can accurately describe the creep characteristics of initial damaged coal sample. Meng et al. [19] provided an innovative variable order fractional model. Compared with the experimental stress-strain data, the model can well study the strain hardening behavior of amorphous glassy polymers.

Euler-Bernoulli beam is widely used in mechanical and manufacturing engineering. The fractional viscoelastic models are used to establish the kinetic equations of Euler-Bernoulli beams. Various methods have been proposed in order to solve kinetic equations. Rahimi et al. [20] described the mechanical deformation of materials with a fractional nonlocal model. The nonlinear kinetic equation of Euler Bernoulli beam is solved by Galerkin weighted residual method. Ali et al. [21] applied the finite difference method to study the in-

hibitory effect of fractional order on Euler-Bernoulli cantilever beam. Oskouie et al. [22] solved the fractional order nonlinear vibration equation of viscoelastic Euler-Bernoulli nanobeam by using Galerkin scheme. Yu et al. [23] solved the fractional order constitutive equation of Euler-Bernoulli beam by using Quasi-Legendre polynomials. The dynamic analysis was carried out with two different viscoelastic materials. Wang et al. [24] solved the polymeric viscoelastic Euler-Bernoulli beam based on Chebyshev polynomials algorithm. It was proved that polynomials algorithm is a valid method for solving fractional beam kinetic equations. An effective algorithm on account of the collocation of shifted Bernstein-Legendre polynomial is applied to numerically solve the viscoelastic Euler-Bernoulli beam in this paper.

Many advanced models have been proposed to investigate the vibration and buckling of different beam structures under compression. Augello et al. [25] built a finite elements method in the framework of the Carrera Unified Formulation (CUF) to evaluate the displacements of the thin walled beams with complex geometric shapes. Zhao et al. [26] proposed a generalized model to study Timoshenko double-beam systems under compressive axial loads. The proposed model was efficient for the forced vibration analysis of the systems. A novel beam theory based on CUF was introduced to discuss the vibration behavior of curved metallic and composite beams [27]. The improved numerical algorithm was used to describe the cross-sectional deformation. Yang et al. [28] developed a refined finite element method based on CUF to investigate the virtual vibration correlation technique for highly flexible thin-walled composite beams.

An accurate and effective numerical algorithm is required to solve the kinetic equations of viscoelastic beams based on variable order fractional model. Polynomial algorithm can directly solve these kinetic equations in time domain. Chen et al. [29] applied generalized fractional Legendre function to solve a fractional differential equation with variable coefficients. They proposed a numerical method to solve a class of variable order nonlinear fractional differential equations based on Legendre wavelet [30]. Hassani et al. [31] proposed a generalized polynomial optimization method for solving variable order fractional nonlinear Klein-Gordon equation.

Bernstein and Legendre polynomials are extensively used to find the solutions of fractional order equations. Among them, Bernstein polynomials have good approximation and stability. Maleknejad et al. [32] used Bernstein polynomials to solve nonlinear Volterra Fredholm Hammerstein integral equation. A type of multi-order fractional differential equations was solved by using Bernstein polynomials method in [33]. The weight function of Legendre polynomials is simpler than other polynomials such as Chebyshev polynomials [34] and Bernoulli polynomials [35]. They have great orthogonality. In this paper, shifted Bernstein polynomials and shifted Legendre polynomials are used to approximate the deflection function of Euler Bernoulli beams.

The paper is organized as follows: Section 2 presents some basic knowledge of variable order fractional differential operators. The kinetic equation of a Euler-Bernoulli beam is established under variable order fractional model.

Section 3 introduces Shifted Bernstein-Legendre polynomial collocation algorithm. In Section 4, numerical examples are given to verify the effectiveness and practicability of the algorithm. Dynamic analysis of viscoelastic beams under different materials and loading conditions is investigated in Section 5. Section 6 gives the conclusions.

2 Preliminaries

This section introduces the definition of variable order fractional differential operators. The kinetic equation of viscoelastic beam is established with variable order fractional model.

2.1 Variable order fractional differential operators

Definition1: Variable order fractional differential operator in Caputo sense (${}^C D_t^{\alpha(t)}$), is defined as follows [36–38]:

$${}^C D_t^{\alpha(t)} f(t) = \frac{1}{\Gamma(1-\alpha(t))} \int_{0+}^t (t-\tau)^{-\alpha(t)} f'(\tau) d\tau \quad (1)$$

where $0 < \alpha(t) \leq 1$ is variable order, $f(t)$ is a continuous function. $\Gamma(*) = \int_0^\infty e^{-t} t^{*-1} dt$ is Gamma function.

According to Eq. (1), when $f(t) = x^m t^n$, it can be gotten:

$${}^C D_t^{\alpha(t)}(x^m t^n) = \begin{cases} 0, n = 0 \\ \frac{\Gamma(n+1)}{\Gamma(n+1-\alpha(t))} t^{n-\alpha(t)} x^m, n = 1, 2, \dots \end{cases} \quad (2)$$

when x^m in Eq. (2) takes 1, the following can be obtained:

$${}^C D_t^{\alpha(t)}(t^n) = \begin{cases} 0, n = 0 \\ \frac{\Gamma(n+1)}{\Gamma(n+1-\alpha(t))} t^{n-\alpha(t)}, n = 1, 2, \dots \end{cases} \quad (3)$$

2.2 Establishment of kinetic equation with variable order fractional model

The variable order fractional kinetic equation of Euler-Bernoulli beam is established. Lateral load exerted on the surface of the beam causes it to bend and deform. The bending deformation is restored to an equilibrium state due to the viscoelasticity of the material, which causes the vertical vibration. Consider a viscoelastic beam with fixed supports at both ends with length of l , width of b and height of h . The configuration of the beam is shown in Fig.1. The deformation of the beam under the distributed load $f(x, t)$.

Kinetic equation of the beam is as follows: [12]:

$$\rho S \frac{\partial^2 w(x, t)}{\partial t^2} + \frac{\partial^2 M(x, t)}{\partial x^2} = f(x, t) \quad (4)$$

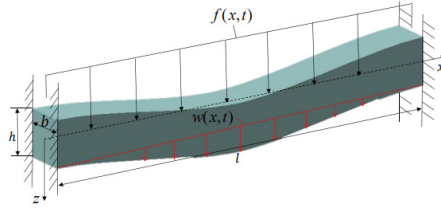


Fig. 1 Configuration of the Euler-Bernoulli beam.

where ρ is density of the viscoelastic beam, S is cross-sectional area. $M(x, t)$ is bending moment. Lateral deflection of the beam is $w(x, t)$.

Bending moment $M(x, t)$ can be expressed as:

$$M(x, t) = \int_S z \sigma(x, t) dz \quad (5)$$

where $\sigma(x, t)$ represents stress, z represents transverse coordinate. The variable order fractional model is proposed by [39]:

$$\sigma(x, t) = E \theta^{\alpha(t)} {}^C D_t^{\alpha(t)} \varepsilon(x, t) \quad (6)$$

where $\varepsilon(t)$ is strain, $\sigma(t)$ is stress. E is Young's modulus, θ represents the relaxation time and ${}^C D_t^{\alpha(t)}(\cdot)$ is defined by Eq. (2), $\alpha(t)$ is variable order.

Stress-deflection relationship of viscoelastic beam can be expressed as:

$$\varepsilon(x, t) = z \frac{\partial^2 w(x, t)}{\partial x^2} \quad (7)$$

Substitute Eq. (5) Eq. (6) and Eq. (7) into Eq. (4), the kinetic equation of Euler-Bernoulli beam is obtained:

$$\rho S \frac{\partial^2 w(x, t)}{\partial t^2} + I E \theta^{\alpha(t)} {}^C D_t^{\alpha(t)} \frac{\partial^4 w(x, t)}{\partial x^4} = f(x, t) \quad (8)$$

where I is inertia.

The fixed boundary conditions at both ends are determined by the following formula:

$$w(0, t) = \frac{\partial w(0, t)}{\partial x} = w(l, t) = \frac{\partial w(l, t)}{\partial x} = 0 \quad (9)$$

The initial condition is written as:

$$w(x, 0) = \frac{\partial w(x, 0)}{\partial t} = 0 \quad (10)$$

3 Bernstein-Legendre polynomial collocation algorithm

The Bernstein Legendre polynomial collocation algorithm will be described in detail to solve the two-dimensional deflection function of the beam. Bernstein polynomial and Legendre polynomial are used for the purpose of approximation basis functions for x and t , respectively. The definition interval of deflection is $[0, R] \times [0, H]$. The main idea is to employ the shifted polynomial as a basic function to precisely approach the unknown deflection function. Matrix items are used to represent the derivative function. The kinetic equation is converted into a matrix product form which is simple to solve.

3.1 Polynomial theory

Definition2: The Bernstein polynomial of $n - th$ is defined as follows [40]:

$$b_{n,i}(x) = \sum_{k=0}^{n-i} (-1)^k \binom{n}{i} \binom{n-i}{k} x^{i+k} \quad (11)$$

where $x \in [0, 1], i = 0, 1, 2, 3, \dots, n$.

The $n - th$ shifted Bernstein polynomial is used to expand the scope of x in $[0, R]$ as:

$$B_{n,i}(x) = \sum_{k=0}^{n-i} (-1)^k \binom{n}{i} \binom{n-i}{k} \frac{1}{R^{i+k}} x^{i+k} \quad (12)$$

A shifted Bernstein polynomials matrix $\Phi(x)$ in $[0, R]$ is expressed as:

$$\Phi(x) = [B_{n,0}(x), B_{n,1}(x), \dots, B_{n,n}(x)]^T \quad (13)$$

Eq. (13) is expressed by the following matrix product:

$$\Phi(x) = AMT_n(x) \quad (14)$$

where

$$A = [a_{i,j}]_{i,j=0}^n, a_{i,j} = \begin{cases} (-1)^{j-i} \binom{n}{i} \binom{n-i}{j-i}, & j \geq i \\ 0, & j < i \end{cases} \quad (15)$$

$$M = [m_{i,j}]_{i,j=0}^n, m_{i,j} = \begin{cases} \frac{1}{R^j}, & j \geq i \\ 0, & j < i \end{cases} \quad (16)$$

$$T_n(x) = [1, x, \dots, x^n]^T \quad (17)$$

A and M are called coefficient matrices of shifted Bernstein polynomials.

$T_n(x)$ can be obtained by:

$$T_n(x) = (AM)^{-1}\Phi(x) \quad (18)$$

Definition3: The $n - th$ Legendre polynomial is defined by [41, 42]:

$$l_{n,i}(t) = \sum_{i=0}^n (-1)^{n+i} \frac{\Gamma(n+i+1)}{\Gamma(n-i+1)(\Gamma(i+1))^2} t^i \quad (19)$$

where $t \in [0, 1]$, $i = 0, 1, 2, 3, \dots, n$. Shifted Legendre polynomial of order n is used to expand the scope of t in $[0, H]$ as:

$$L_{n,i}(t) = \sum_{i=0}^n (-1)^{n+i} \frac{\Gamma(n+i+1)}{\Gamma(n-i+1)(\Gamma(i+1))^2} \left(\frac{1}{H}\right)^i t^i \quad (20)$$

A shifted Legendre polynomials matrix $\Theta(t)$ in $[0, H]$ is expressed as:

$$\Theta(t) = [L_{n,0}(t), L_{n,1}(t), \dots, L_{n,n}(t)]^T \quad (21)$$

Eq. (21) can be indicated by the following matrix product:

$$\Theta(t) = PNT_n(t) \quad (22)$$

where

$$P = [A_{i,j}]_{i,j=0}^n, A_{i,j} = \begin{cases} 0, & j > i \\ (-1)^{i+j} \frac{\Gamma(i+j+1)}{\Gamma(i-j+1)(\Gamma(j+1))^2}, & j \leq i \end{cases} \quad (23)$$

$$N = \begin{cases} 0, & j \neq i \\ \frac{1}{H^i}, & j = i \end{cases} \quad (24)$$

$$T_n(t) = [1, t, \dots, t^n]^T \quad (25)$$

T_n can be rewritten as:

$$T_n(t) = (PN)^{-1}\Theta(t) \quad (26)$$

3.2 Approximation of unknown function

A continuous function $w(x)$, $x \in [0, R]$ is approximated by shifted Bernstein polynomial as:

$$\begin{aligned} w(x) &= \lim_{n \rightarrow \infty} \sum_{i=0}^n c_i B_{n,i}(x) \\ &\approx \sum_{i=0}^n c_i B_{n,i}(x) \\ &= C^T \Phi(x) \end{aligned} \quad (27)$$

where $C^T = [c_0, c_1, \dots, c_n]$.

The calculation is as following:

$$\begin{aligned} \langle w(x), \Phi^T(x) \rangle &= C^T \langle \Phi(x), \Phi^T(x) \rangle \\ &= C^T Q \end{aligned} \quad (28)$$

where $Q = \langle \Phi(x), \Phi^T(x) \rangle = [q_{i,j}]_{i,j=0}^n$, $q_{i,j} = \int_0^R B_{n,i}(x)B_{n,j}(x)dx$, $C^T = \langle w(x), \Phi^T(x) \rangle > Q^{-1}$.

Similarly, $w(t), t \in [0, H]$ can be approximated by shifted Legendre polynomial as:

$$\begin{aligned} w(t) &= \lim_{n \rightarrow \infty} \sum_{i=0}^n k_i L_{n,i}(t) \\ &\approx \sum_{i=0}^n k_i L_{n,i}(t) \\ &= K^T \Theta(t) \end{aligned} \quad (29)$$

where $K^T = [k_0, k_1, \dots, k_n]$.

Similarly, the following results is obtained:

$$\begin{aligned} \langle w(t), \Theta^T(t) \rangle &= K^T \langle \Theta(t), \Theta^T(t) \rangle \\ &= K^T Y \end{aligned} \quad (30)$$

where $Y = \langle \Theta(t), \Theta^T(t) \rangle = [y_{i,j}]_{i,j=0}^n$, $y_{i,j} = \int_0^H L_{n,i}(t)L_{n,j}(t)dt$ and so $K^T = \langle w(t), \Theta^T(t) \rangle > Y^{-1}$.

Binary function $w(x, t) \in L^2([0, R] \times [0, H])$ is approximated to the following form [43]:

$$\begin{aligned} w(x, t) &= \lim_{n \rightarrow \infty} \sum_{j=0}^n \left(\sum_{i=0}^n c_i B_{n,i}(x) \right) k_j L_{n,j}(t) \\ &\approx \sum_{j=0}^n \sum_{i=0}^n B_{n,i}(x) c_i k_j L_{n,j}(t) \\ &= \Phi^T(x) W \Theta(t) \end{aligned} \quad (31)$$

where $W = [w_{i,j}]_{i,j=0}^n$, $w_{i,j} = c_i k_j$.

3.3 Integer order differential operational matrix

Definition4: G is called first-order shifted Bernstein differential operational matrix if G satisfies $\Phi'(x) = G\Phi(x)$.

$$\begin{aligned} \Phi'(x) &= \frac{dAMT_n(x)}{dx} = AM \frac{dT_n(x)}{dx} \\ &= AMVT_n(x) = AMV(AM)^{-1}\Phi(x) \\ &= G\Phi(x) \end{aligned} \quad (32)$$

where

$$V = [v_{i,j}]_{i,j=0}^n, v_{i,j} = \begin{cases} i, & i = j + 1 \\ 0, & i \neq j + 1 \end{cases} \quad (33)$$

$G = AMV(AM)^{-1}$ is first-order differential operational matrix. Finding n -th derivative in Eq. (34) as the following formula:

$$\Phi^{(n)}(x) = G^n \Phi(x) \quad (34)$$

According to Eq. (31) and Eq. (34), the following equations are obtained:

$$\frac{\partial^n w(x, t)}{\partial x^n} \approx \frac{\partial^n (\Phi^T(x) W \Theta(t))}{\partial x^n} = \left(\frac{\partial^n \Phi(x)}{\partial x^n} \right)^T W \Theta(t) = \Phi^T(x) (G^T)^n W \Theta(t) \quad (35)$$

Definition5: If there is the matrix Ω satisfying $\Theta'(t) = \Omega \Theta(t)$, Ω is called the first-order shifted Legendre differential operational matrix.

$$\begin{aligned} \Theta'(t) &= \frac{dPNT_n(t)}{dt} = PN \frac{dT_n(t)}{dt} \\ &= PNV T_n(t) = PNV(PN)^{-1} \Theta(t) \\ &= \Omega \Theta(t) \end{aligned} \quad (36)$$

where $\Omega = PNV(PN)^{-1}$ is a first-order differential operational matrix. The following formula is obtained:

$$\Theta^{(n)}(t) = \Omega^n \Theta(t) \quad (37)$$

Above all, the following formula is obtained:

$$\frac{\partial^n w(x, t)}{\partial t^n} \approx \frac{\partial^n (\Phi^T(x) W \Theta(t))}{\partial t^n} = \Phi^T(x) W \left(\frac{\partial^n \Theta(t)}{\partial t^n} \right) = \Phi^T(x) W \Omega^n \Theta(t) \quad (38)$$

3.4 Variable order fractional differential operational matrix

Definition6: If there is the matrix ϕ satisfying ${}^C D_t^{\alpha(t)} \Theta(t) = \phi \Theta(t)$, ϕ is called variable order fractional differential operational matrix.

$$\begin{aligned} {}^C D_t^{\alpha(t)} \Theta(t) &= {}^C D_t^{\alpha(t)} (PNT_n(t)) = PN {}^C D_t^{\alpha(t)} (T_n(t)) \\ &= PNF T_n(t) = PNF(PN)^{-1} \Theta(t) \\ &= \phi \Theta(t) \end{aligned} \quad (39)$$

where

$$F = [f_{i,j}]_{i,j=0}^n, f_{i,j} = \begin{cases} \frac{\Gamma(i+1)}{\Gamma(i+1-\alpha(t))} t^{-\alpha(t)}, & i = j \neq 0 \\ 0, & \text{else} \end{cases} \quad (40)$$

$$\phi = PNF PN^{-1} \quad (41)$$

On the basis of Eq. (35) and Eq. (39), the following equations can be obtained:

$$\begin{aligned}
{}^C D_t^{\alpha(t)} \frac{\partial^n w(x, t)}{\partial x^n} &\approx {}^C D_t^{\alpha(t)} \frac{\partial^n (\Phi^T(x) W \Theta(t))}{\partial x^n} \\
&= \left(\frac{\partial^n \Phi(x)}{\partial x^n} \right)^T W {}^C D_t^{\alpha(t)} \Theta(t) \\
&= \Phi^T(x) (G^T)^n W \phi \Theta(t)
\end{aligned} \tag{42}$$

Substituting Eq. (38) and Eq. (42) into Eq. (8), the following formula can be obtained:

$$\rho S \Phi^T(x) W \Omega^2 \Theta(t) + I E \theta^{r(t)} \Phi^T(x) (G^T)^4 W \phi \Theta(t) = f(x, t) \tag{43}$$

The initial conditions in Eq. (9) and boundary conditions in Eq. (10) can be rewritten as:

$$\begin{aligned}
\Phi^T(0) W \Theta(t) &= \Phi^T(0) G W \Theta(t) = 0 \\
\Phi^T(l) W \Theta(t) &= \Phi^T(l) G W \Theta(t) = 0 \\
\Phi^T(x) W \Theta(0) &= \Phi^T(x) W \Omega \Theta(0) = 0
\end{aligned} \tag{44}$$

Variable (x, t) is discretized into (x_i, t_j) , according to the collection method. Eq. (43) is transformed into a set of algebraic equations by selecting nodes. $w_{i,j}$ can be obtained through mathematical software. Ultimately, the time-domain numerical solutions of variable order fractional partial differential equations are obtained.

4 Numerical analysis

In this part, a general mathematical example is given to demonstrate the effectiveness of the algorithm. Then, the proposed algorithm is applied to solve the kinetic equation of HDPE beam, and compared with the solution based on fractional order model. It shows that the proposed algorithm can simplify the iteration steps. The variable order fractional model exhibits fewer material parameters and a wider range of applications than the constant fractional model.

4.1 Mathematical example

A mathematical in the same structure as the kinetic equation with variable order fractional mode is proposed in this part. The effectiveness of the method is verified by a mathematical example of the analytical solution.

$$\frac{\partial^2 w(x, t)}{\partial t^2} + {}^C D_t^{\alpha(t)} \frac{\partial^4 w(x, t)}{\partial x^4} = f(x, t) \tag{45}$$

$$w(0, t) = \frac{\partial w(0, t)}{\partial x} = 0, w(1, t) = \frac{\partial w(1, t)}{\partial x} = 0 \tag{46}$$

$$w(x, 0) = 0, \frac{\partial w(x, 0)}{\partial t} = 0 \quad (47)$$

where $\alpha(t) = -0.1t + 1, t \in [0, 1]$. $f(x, t) = 2x^2(1-x)^2 + 24\frac{\Gamma(3)}{\Gamma(3-r(t))}t^{2-\alpha(t)}$. The analytical solution is $w(x, t) = x^2(1-x)^2t^2$.

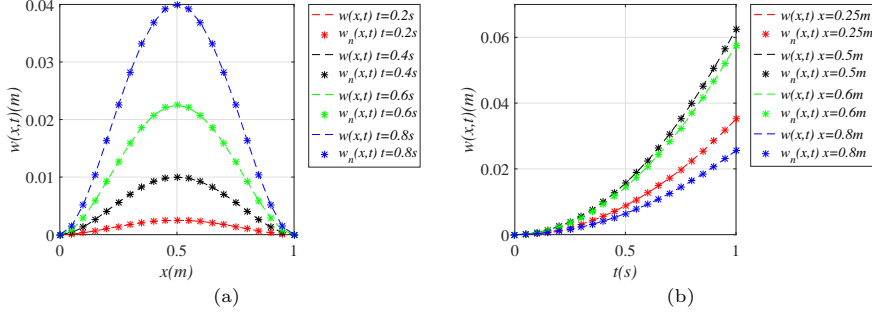


Fig. 2 Comparison of $w_n(x, t)$ and $w(x, t)$: (a) for different values of t (b) for different values of x .

Using the shifted Bernstein-Legendre polynomial collocation algorithm, the numerical solution $w_n(x, t)$ with the number of items of 4 is obtained. The numerical solutions at various t and x are obtained, as shown in Fig. 2. The effectiveness of this algorithm is verified by comparison with the analytical solution.

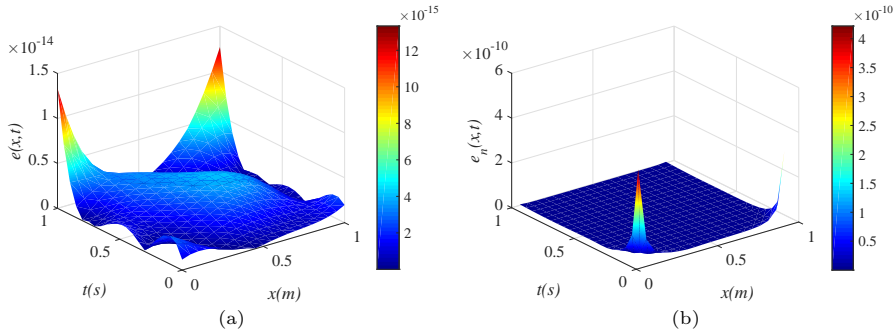


Fig. 3 (a) The absolute error $e(x, t)$ and (b) the relative error $e_n(x, t)$.

Fig. 3 shows $e(x, t)$ and $e_n(x, t)$ at some points when $n = 4$. where

$$e(x, t) = |w_n(x, t) - w(x, t)| \quad (48)$$

$$e_n(x, t) = \frac{|w_n(x, t) - w(x, t)|}{w(x, t)} \quad (49)$$

The absolute error can reach 10^{-14} in Fig. 3(a), which presents the high accuracy of the proposed algorithm. The relative error is explained in order to better reflect the reliability of the calculation results. The relative error can reach 10^{-10} in Fig. 3(b), which confirms the high efficiency of the proposed algorithm.

4.2 Deflection solution of viscoelastic high density polyethylene (HDPE) beam

Wang and Chen [43] used Chebyshev polynomial approximation theory to calculate the bending vibration equation of viscoelastic beams with fractional order model. Fractional order is replaced by a function of t in this part. The bending vibration equation of HDPE beams is generalized as a variable order fractional equation. The shifted Bernstein-Legendre polynomial collocation algorithm is used to calculate the deflection of HDPE beam. The parameters in the bending vibration equation of HDPE beam are involved in Table 1 [43].

Material	ρ_1	A_1	E_1	I_1	Ω_1
HDPE	960 kg/m ³	0.04 m ²	3.341×10^9 Pa	0.0016/12 m ⁴	$\pi/2$

Table 1 Material properties of the beam considered in numerical computation.

HDPE beam bending vibration equation is given by:

$$\rho_1 A_1 \frac{\partial^2 w(x, t)}{\partial t^2} + E_1 I_1 {}^C D_t^{\alpha(t)} \frac{\partial^4 w(x, t)}{\partial x^4} - \rho_1 A_1 \Omega_1^2 x \frac{\partial^2 w(x, t)}{\partial x^2} = f(x, t) \quad (50)$$

$$\begin{cases} w(0, t) = \frac{\partial w(0, t)}{\partial x} = 0 \\ \frac{\partial^2 w(l, t)}{\partial x^2} = \frac{\partial^3 w(l, t)}{\partial x^3} = 0 \\ w(x, 0) = 0, \frac{\partial w(x, 0)}{\partial t} = 0 \end{cases} \quad (51)$$

where variable fraction order $\alpha(t) = -0.1t + 1$, $t \in [0, 1]$, ρ_1 is density of HDPE, A_1 is cross-sectional area of rotating beam, E_1 is parameter, I_1 is the moment, Ω_1 is the rotation speed of the beam, $w(x, t)$ is deflection and $f(x, t)$ is load.

Shifted Bernstein-Legendre polynomial collocation algorithm can be used to find the numerical solution of deflection under $f(x, t) = 10$ N/m, $f(x, t) = 10\pi \sin t$ N/m and $f(x, t) = (10 + 2x)$ N/m.

According to Fig. 4, Lateral deflection of viscoelastic HDPE beam is calculated by the proposed algorithm. The variable order values from 0 to 1 reflect the behavior of materials from pure elasticity to pure viscosity. The value of the variable order does not change with the position x . Therefore, a linear function of t is proposed for the variable order. Meng et al. presented variable order fractional and fractional order models to describe the stress evolution

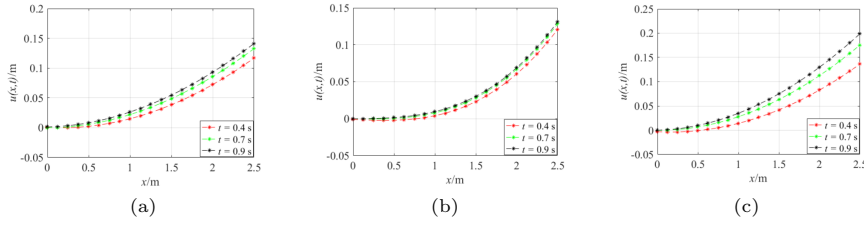


Fig. 4 Deflection of HDPE beam under three types of loading conditions: (a) $f(x, t) = 10 \text{ N/m}$ (b) $f(x, t) = 10\pi \sin t \text{ N/m}$ (c) $f(x, t) = (10 + 2x) \text{ N/m}$.

of viscoelastic materials [19]. It showed that variable order fractional model can better describe the dynamic response under large strain. The numerical solution of the mathematical example is obtained. The absolute error of the example can reach 10^{-14} , which presents the high accuracy of the algorithm. Compared with reference [43], the deflection increases gradually with the decrease of variable order. It indicates that the variable order affects the dynamic response of the viscoelastic materials. Viscoelastic model with variable order fractional is more sensitive compared with the viscoelastic model with constant fractional order.

5 Dynamic analysis of viscoelastic Euler-Bernoulli beam

The dynamic response of viscoelastic beams under different loading conditions is analyzed numerically. It is worth noting that the numerical algorithm in this section selects n as 4. The deflection $w(x, t)$, strain $\varepsilon(x, t)$ and stress $\sigma(x, t)$ of the viscoelastic beam are calculated.

Meng et al. [39] analysed the stress-strain response of the polymers under large deformation by using variable order fractional viscoelastic model. Material parameters determined in the polyurea and PET models are shown in Table 2.

In Table 2, the function $\alpha(t)$ was proposed by Meng et al. [19], which was selected according to the viscoelasticity of the material. It is proved that the time-varying linear variable order fractional function is suitable to describe the strain hardening behavior of polymers.

Beam	E	ρ	$\alpha(t)$	θ
Polyurea	$1.2 \times 10^8 \text{ Pa}$	1060 kg/m^3	$-0.1t + 1$	0.0012 s
PET	$3 \times 10^7 \text{ Pa}$	1380 kg/m^3	$-0.1t + 1$	0.35 s

Table 2 Material properties of polyuria and PET.

5.1 Dynamic analysis of polyurea beam

The geometrical parameters of the beam are represented in Table 3. The parameters of polyurea and beam are substituted into Eqs. (8)-(10). The solution of the kinetic equation is solved by Bernstein-Legendre polynomial collocation algorithm.

l	b	h	I	S
5 m	0.1 m	0.1 m	$0.1^4/12 \text{ m}^4$	0.01 m^2

Table 3 Geometrical parameters of the beam.

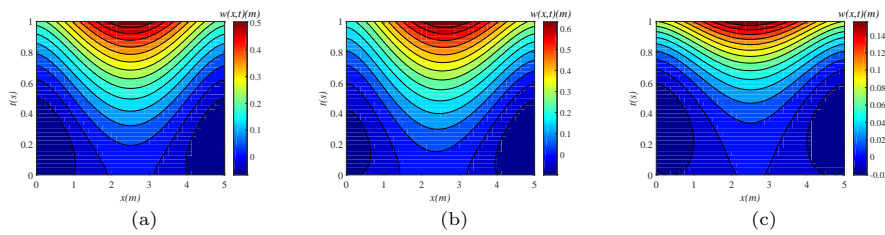


Fig. 5 Deflection of polyurea beam under various loads: (a) $f(x, t) = 10 \text{ N/m}$ (b) $f(x, t) = (10 + x) \text{ N/m}$ (c) $f(x, t) = 10 \sin t \text{ N/m}$.

Fig. 5 shows the change of the deflection of the polyurea beam under uniform load, linear load and harmonic load. Lateral deflection increases with the value of x and t . The maximum deflection value can be reached at the midpoint of beam. The deflection is symmetrical with respect to $x = 2.5 \text{ m}$. As shown in Fig. 5 (a), the deflection of the beam shows the same trend under different loading conditions. Similar results are observed in Fig. 5(b) and 5(c).

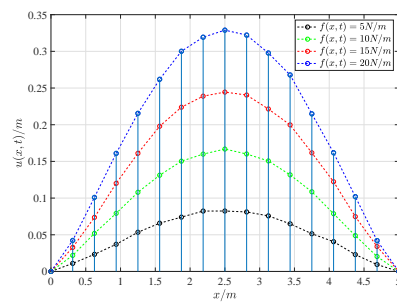


Fig. 6 Deflection of polyurea beam under uniform loads.

The sensitivity of the loading parameters on the deflection of the viscoelastic is studied in this part. The uniform load with various load values is applied on the beam. Fig. 6 shows the deflection variation under different uniformly distributed load values. The deflection of the beam is symmetrical about the middle for each uniform load value. The deflection increases as the uniform load value increases.

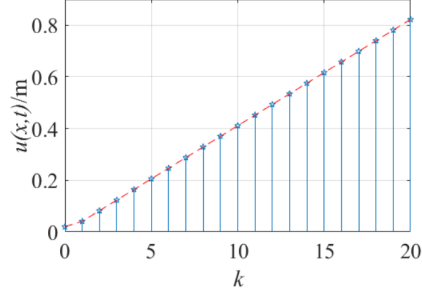


Fig. 7 Maximum deflection of polyurea beam under different parameter k of linear loads.

Linear loads of different slopes are applied to the beam. Fig. 7 represents the maximum deflection of the beam at $x = 2.5$ m with different slope k of linear load $f(x, t) = (10 + kx)$ N/m. It can be observed from the figure that the deflection of the beam increases linearly with the increase of slope k .

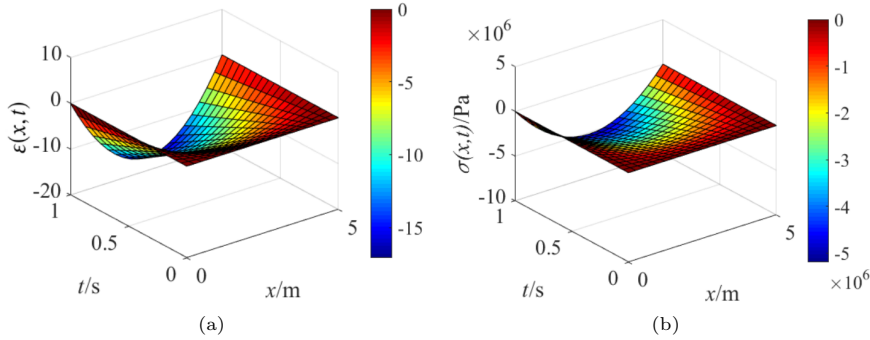


Fig. 8 (a) Strain and (b) Stress of the viscoelastic beam under uniform load $f(x, t) = 10$ N/m.

Three-dimensional curves of stress and strain values of viscoelastic beam with time and position under uniform load is shown in Fig. 8. The initial and boundary conditions are well respected in the numerical results. The stress and strain reach the maximum value at $x = 2.5$ m, which is consistent with the previously observed beam deflection.

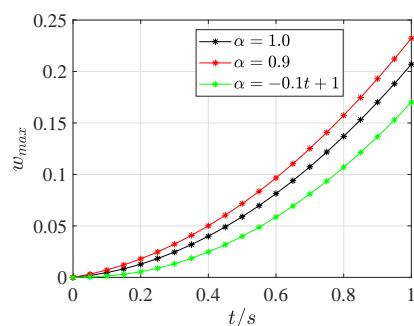


Fig. 9 Maximum deflection of polyurea beam under $f(x, t) = 10 \text{ N/m}$ with integer order, constant and variable fractional order.

Fig. 9 shows the evolution of the maximum deflection of viscoelastic polyurea beam in function of time with different values of order: including integer order $\alpha = 1$, constant fractional order $\alpha = 0.9$ and variable fractional order $\alpha = -0.1t + 1$. The same uniformly distributed load $f(x, t) = 10 \text{ N/m}$ is applied on the beam. The deflection of the beam is compared with different orders. For all the three orders, the deflection of the beam increases with time. The deflection of the beam with variable fractional order is smaller than those with integer order and constant fractional order.

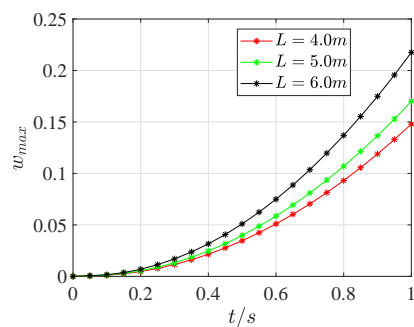


Fig. 10 Maximum deflection of polyurea beam of different length with the variable fractional order under $f(x, t) = 10 \text{ N/m}$.

Fig. 10 shows the evolution of the maximum deflection of viscoelastic polyurea beams of different length in function of time. The variable fractional order viscoelastic model is applied on the beams, which are under uniformly distributed load. It indicates that the maximum deflection of the beam increases with its length.

The deflection of the beam with length 1 m under the same uniformly distributed load $f(x, t) = 10 \text{ N/m}$ with different variable fractional order is shown in Fig. 11. The difference of the variable fractional order is the coefficient in

front of t and loading time. It confirms that the deflection of the beam with the same loading time is coherent with different variable fractional order. The deflection of the beam increases with the loading time.

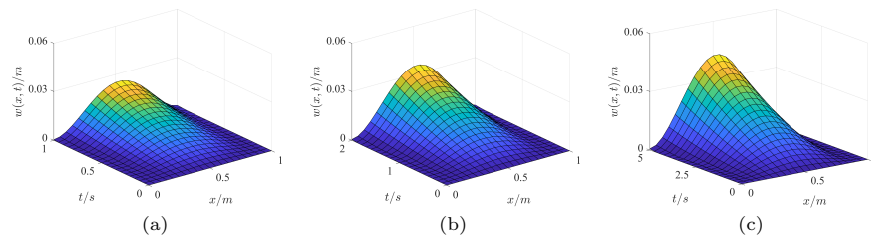


Fig. 11 Deflection of polyurea beam under different types of variable order fractional model with different loading time : (a) $\alpha(t) = -0.1t + 1, t \in [0, 1]$ (b) $\alpha(t) = -0.05t + 1, t \in [0, 2]$ (c) $\alpha(t) = -0.02t + 1, t \in [0, 5]$.

5.2 Comparison with different materials

In the study, two kinds of polymer materials are used to study the effect of material properties on the deflection of viscoelastic beams. The material parameters of polyurea and PET are summarized in Table 2. These parameters are applied into Eqs. (8)-(10) to obtain the kinetic equations. The proposed algorithm is used to calculate the deflection.

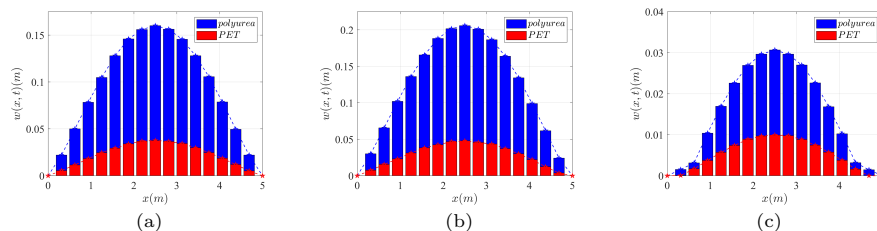


Fig. 12 Comparison of deflection between polyurea and PET beam: (a) $f(x, t) = 10 \text{ N/m}$ (b) $f(x, t) = (10 + x) \text{ N/m}$ (c) $f(x, t) = 10 \sin t \text{ N/m}$.

The deflection changes of polyurea and PET beams under different loads are shown in Fig. 12. Under the same load, the deflection of PET beam is less than that of polyurea beam. The PET beam exhibits better flexural properties than polyurea beam. The results obtained are consistent with the mechanical properties of the material. The conclusion is conformed to the actual situation, which indicates the precision of the algorithm.

6 Conclusions and perspectives

An accurate numerical algorithm for solving kinetic equations of viscoelastic Euler-Bernoulli beams is proposed with variable order fractional model. The algorithm is developed with shifted Bernstein and Legendre polynomial and it can be used to obtain directly the numerical solution in time domain. Among the results, the main finding can be summarized as follows:

(1) Variable order fractional model reduces the number of physical parameters and better describes the damping characteristics of viscoelastic beams.

(2) Effectiveness and practicability of the algorithm are verified by mathematical examples.

(3) Viscoelastic model with variable order fractional exhibits better sensitivity compared to the viscoelastic model with fractional order model.

(4) The deflection numerical solution of polyurea beam under different loads is investigated. The maximum deflection is found in the middle of the beam.

(5) PET beams have better flexural properties than polyurea beams.

The effectiveness of the proposed polynomial algorithm is validated for Euler-Bernoulli beams with linear load conditions. The nonlinear vibrations of the beams with viscoelastic model will be effectuated in the future. Other nonlinear viscoelastic models will be used to describe the complex mechanical behaviors of the materials.

Acknowledgements

This work is supported by the National Natural Science Foundation (52074126) in China and the LE STUDIUM RESEARCH PROFESSORSHIP award of Centre-Val de Loire region in France.

References

1. Pu H, Liu T, Yang Z, Synthesis and application of polyurea, *Polym. Mater. Sci. Eng.* 24(7)(2008) 1–5.
2. Huang H, Yan H, Fu H, Preparation of microcapsules and their application in daily chemicals, *Chem. Bioen.* 27(2010) 10–12.
3. Struik L C E, Free damped vibrations of linear viscoelastic materials, *Rheo. Act.* 6(2)(1967) 119–129.
4. Pipkin A C, *Lectures on viscoelasticity theory*, New York, 1972.
5. Flügge W, *Viscoelasticity*, New York, 1975.
6. Christensen R M, *Theory of viscoelasticity : an introduction (2nd)*, New York, 1982.
7. Oskouie M F, Ansari R, Linear and nonlinear vibrations of fractional viscoelastic Timoshenko nanobeams considering surface energy effects, *Appl Math Model.* 43(2017) 337-350.
8. Oskouie M F, Ansari R, Rouhi H, Vibration analysis of FG nanobeams on the basis of fractional nonlocal model: a variational approach, *Microsyst Technol.* 24(2018) 2775-2782.

9. Oskouie M F, Ansari R, Rouhi H, Nonlinear bending and postbuckling analysis of FG nanoscale beams using the two-phase fractional nonlocal continuum mechanics, *Eur. Phys. J. Plus.* 134(2019) 1-15. Christensen R M, Theory of viscoelasticity : an introduction (2nd), New York, 1982.
10. Xu J, Chen YD, Tai YP, Xu XM, Shi GD, Chen N, Vibration analysis of complex fractional viscoelastic beam structures by the wave method, *Int. J. Mech. Sci.* 167(2020) 105204.
11. Freundlich J, Transient vibrations of a fractional Kelvin-Voigt viscoelastic cantilever beam with a tip mass and subjected to a base excitation, *J. Soud. Vib.* 438(2019) 99–115.
12. Martin O, Stability approach to the fractional variational iteration method used for the dynamic analysis of viscoelastic beams, *J. Comput. Appl. Math.* 346(2019) 261–276.
13. Loghman E, Bakhtiari-Nejad F, Kamali A, Abbaszadeh M, Nonlinear vibration of fractional viscoelastic micro-beams, *Int J. Nonlin Mech.* 137(2021) 103811.
14. Liu X, Li D, A link between a variable-order fractional Zener model and non-Newtonian time-varying viscosity for viscoelastic material: relaxation time, *Acta Mech.* 232(1)(2021) 1-13.
15. Burlon A, Alotta G, Di Paola M, Failla G, An original perspective on variable-order fractional operators for viscoelastic materials, *Meccanica.* 56(4)(2021) 769-784.
16. Ramirez L E S, Coimbra C F M, On the variable order dynamics of the nonlinear wake caused by a sedimenting particle, *Physica. D.* 240(13)(2011) 1111–1118.
17. Sun L, Chen YM, Numerical analysis of variable order fractional viscoelastic column based on two-dimensional Legendre wavelets algorithm, *Chaos Solitons Fractals.* 152(2021) 111372.
18. Huang P, Zhang J, Jean Damascene N, Dong C, Wang Z, A fractional order viscoelastic-plastic creep model for coal sample considering initial damage accumulation, *Alexandria Engineering Journal.* 60(4)(2021) 3921-3930.
19. Meng R, Yin D, Yang H, Xiang J, Parameter study of variable order fractional model for the strain hardening behavior of glassy polymers, *Physica A.* 545(2020) 123763.
20. Rahimi Z, Sumelka W, Yang X J, A new fractional nonlocal model and its application in free vibration of Timoshenko and Euler-Bernoulli beams, *Eur. Phys. J. Plus.* 132(11)(2017) 1–10.
21. Ali M, Khan M W, Abid M, Rehman AU, Variation of fraction in FOPID controller for vibration control of Euler-Bernoulli beam, *SN Applied Sciences.* 2(12)(2020) 1–9.
22. Oskouie M F, Ansari R, Sadeghi F, Nonlinear vibration analysis of fractional viscoelastic Euler-Bernoulli nanobeams based on the surface stress theory, *Acta Mechanica Solida Sinica.* 30(4)(2017) 416–424.
23. Yu CX, Zhang J, Chen YM, Feng YJ, Yang AM, A numerical method for solving fractional-order viscoelastic Euler-Bernoulli beams, *Chaos, solitons and fractals.* 128(2019) 275–279.
24. Wang L, Chen YM, Cheng G, Barriere T, Numerical analysis of fractional partial differential equations applied to polymeric visco-elastic Euler-Bernoulli beam under quasi-static loads, *Chaos, solitons and fractals.* 140(2020) 110255.
25. Augello R, Daneshkhah E, Xu X, Carrera E, Efficient CUF-based method for the vibrations of thin-walled open cross-section beams under compression, *J Sound Vib.* 510(2021) 116232.
26. Zhao X, Chen B, Li Y H, Zhu W D, Nkiegaing F J, Shao Y B, Forced vibration analysis of Timoshenko double-beam system under compressive axial load by means of Green's functions, *J Sound Vib.* 464(2020) 115001.
27. Yan Y, Carrera E, Pagani A, Free vibration analysis of curved metallic and composite beam structures using a novel variable-kinematic DQ method, *Mech. Adv. Mater. Struct.* (2021) 1-27.
28. Yang H, Daneshkhah E, Augello R, Xu X, Carrera E. Numerical vibration correlation technique for thin-walled composite beams under compression based on accurate refined finite element, *Compos Struct.* 280(2022) 114861.
29. Chen YM, Sun YN, Liu LQ, Numerical solution of fractional partial differential equations with variable coefficients using generalized fractional order Legendre functions, *Appl. Math. Lett.* 244(2014) 847–858.

30. Chen YM, Wei YQ, Liu DY, Yu H, Numerical solution for a class of nonlinear variable order fractional differential equations with Legendre wavelets, *Appl. Math. Lett.* 46(2015) 83–88.
31. Hassani H, Machadob J A T, Naraghirad E, An efficient numerical technique for variable order time fractional nonlinear Klein-Gordon equation, *Appl. Numer. Math.* 154(2020) 260–272.
32. Maleknejad K, Hashemizadeh E, Basirat B, Computational method based on Bernstein operational matrices for nonlinear Volterra-Fredholm-Hammerstein integral equations, *Commun. Nonlinear. Sci.* 17(1)(2012) 52–61.
33. Rostamy D, Jafari H, Alipour M, Khaliq CM, Computational method based on Bernstein operational matrices for multi-order fractional differential equations, *Filomat.* 28(3)(2014) 591–601.
34. Huang YX, Zhao Y, Wang TS, Tian H, A new chebyshev spectral approach for vibration of in-plane functionally graded mindlin plates with variable thickness, *Appl. Math. Model.* 74(2019) 21–42.
35. Ren QW, Tian HJ, Numerical solution of the static beam problem by Bernoulli collocation method, *Appl. Math. Model.* 40(21–22)(2016) 8886–8897.
36. Coimbra C F M, Mechanics with variable-order differential operators, *Ann. Phys-Berlin.* 12(11–12)(2003) 692–703.
37. Oskouie M F, Ansari R, Rouhi H, Bending analysis of functionally graded nanobeams based on the fractional nonlocal continuum theory by the variational Legendre spectral collocation method, *Meccanica.* 53(4)(2017) 1115–1130.
38. Nutting P G, A study of elastic viscous deformation, *Proceedings American Soc. For a Testing Materials.* 21(1921) 1162–1171.
39. Meng R, Yin D, Drapaca C S, A variable order fractional constitutive model of the viscoelastic behavior of polymers, *Int. J. Nonlin. Mech.* 113(2019) 171–177.
40. Mirzaee F, Samadyar N, Application of orthonormal Bernstein polynomials to construct a efficient scheme for solving fractional stochastic integro-differential equation, *Optik.* 132(2017) 262–273.
41. Xu Y, Zhang YM, Zhao JJ, Error analysis of the Legendre-Gauss collocation methods for the nonlinear distributed-order fractional differential equation, *Appl. Numer. Math.* 142(2019) 122–138.
42. Safaie E, Farahi M H, Ardehaie M F, An approximate method for numerically solving multi-dimensional delay fractional optimal control problems by Bernstein polynomials, *Comput. Appl. Math.* 34(3)(2015) 831–846.
43. Wang L, Chen YM, Shifted-Chebyshev-polynomial-based numerical algorithm for fractional order polymer visco-elastic rotating beam, *Chaos, solitons and fractals.* 132(2020) 109585.

Table 4 Nomenclature

Symbol	Explanation
${}^C D_t^{r(t)}$	Variable fraction differential operator
$r(t)$	variable order fractional
$\Gamma(\cdot)$	Gamma function
l	Length of fixed beam at both ends
b	Width
h	Height
z	Transverse coordinate
$M(x, t)$	Bending moment
S	Cross-sectional area
ρ	Density of the viscoelastic material
$\sigma(x, t)$	Stress
$\varepsilon(x, t)$	Strain
x	Position
t	Time
E	Young's modulus
θ	Parameters of viscoelastic materials
η	Viscosity of the material
I	Area moment of inertia
$b_{n,i}(x), l_{n,i}(t)$	Basis function
$B_{n,i}(x), L_{n,i}(t)$	Shifted basis function
A, M	Coefficient matrices of shifted Bernstein polynomials
P, N	Coefficient matrices of shifted Legendre polynomials
C	Coefficient vector of shifted Bernstein polynomials approximation to $w(x)$
K	Coefficient vector of shifted Legendre polynomials approximation to $w(t)$
W	Coefficient vector of shifted Bernstein-Legendre polynomials approximation to $w(x, t)$
$\Phi(x), \Theta(t)$	Family of shifted polynomials
n	Polynomial degree
G	First order operational matrix with respect to x
Ω	First order operational matrix with respect to t
ϕ	variable order fractional operational matrix
$w(x, t)$	Analytical solution
$w_n(x, t)$	Numerical solution
$e(x, t)$	Absolute error
$e_n(x, t)$	Relative error
HDPE	High density polyethylene
ρ_1	Density of HDPE
A_1	Cross-sectional area of HDPE beam
E_1	Parameter of HDPE beam
I_1	Inertia of HDPE beam
Ω_1	Rotation speed of HDPE beam
$f(x, t)$	Distributed load